Supporting information

Novel tetranuclear Pd^{II} and Pt^{II} anticancer complexes derived from pyrene thiosemicarbazones

Carolina G. Oliveira[a,b,c*], Isolda Romero-Canelón[d], James P. C. Coverdale[c], Pedro Ivo S. Maia[e], Guy J. Clarkson[c], Victor M. Deflon[a*] and Peter J. Sadler[c*]

[a] São Carlos Institute of Chemistry, University of São Paulo, 13560-970, São Carlos, Brazil
[b] Institute of Chemistry, Federal University of Uberlândia, 38400-902, Uberlândia, Brazil
[c] Department of Chemistry, University of Warwick, CV4 7AL, Coventry, United Kingdom
[d] School of Pharmacy, University of Birmingham, B15 2TT, Birmingham, United Kingdom
[e] Department of Chemistry, Federal University of the Triângulo Mineiro, 38025-440, Uberaba, Brazil

carolina@ufu.br, P.J.Sadler@warwick.ac.uk and deflon@usp.br

Table of contents

X-ray crystallography

Determination of crystal structure of $[Pt_4(\mu\text{-S-PrCh-}\kappa^3\text{-}C,N,S)_4]\cdot(CH_3)_2CO\cdot CHCl_3$ (4)

Deposited at the Cambridge Crystallographic Data Centre under the accession number CCDC 1990070.

Voids located by the Squeeze routine are output below:

```
# SQUEEZE RESULTS (Version = 11015)
# Note: Data are Listed for all Voids in the P1 Unit Cell
# i.e. Centre of Gravity, Solvent Accessible Volume,
# Recovered number of Electrons in the Void and
# Details about the Squeezed Material
loop_
  _platon_squeeze_void_number
  _platon_squeeze_void_average_x
  _platon_squeeze_void_average_y
  _platon_squeeze_void_average_z
  _platon_squeeze_void_volume
  _platon_squeeze_void_count_electrons
  _platon_squeeze_void_content
   1  0.113  0.489  0.720       542       166 ' '
   2 -0.113  0.511  0.280       543       167 ' '
   3  0.387 -0.011  0.780       543       167 ' '
   4  0.613  0.011  0.220       541       166 ' '
_platon_squeeze_void_probe_radius: 1.20
```

The unit cell contains voids that correlate with about 8 chloroform and 4 acetone molecules (roughly 2 chloroforms and one acetone per void based on a volume of about 150 angstroms cubed per solvent and an electron count of 58 electrons for chloroform and 32 for acetone (that would be a volume of about 450 $Å^3$ and 148 electrons per void) each) which have been treated as a diffuse contribution to the overall scattering without specific atom positions by SQUEEZE/PLATON.

The NHs were placed at calculated positions. Several DFIX, DANG and SIMU restraints were used to give the disordered components reasonable bond lengths, angles and thermal parameters. Some of the NHs have short contacts to acetone solvent and there is a short contact from an acetone to a solvent chloroform. Short contacts are tabulated below: Specified hydrogen bonds (with esds except fixed and riding H).

D-H	H...A	D...A	<(DHA)	
0.88	2.21	3.040(16)	158.3	N221-H221...O5
0.88	2.13	2.994(14)	167.2	N121-H121...O2
1.00	2.58	3.40(3)	139.4	C10-H10...O2

There is possible π-stacking, but there is only a very slight overlap between the pyrene rings. Their orientation may be dominated by the requirements of coordination. These are characterized by the atoms used to define mean planes, angle between these mean planes and closest atomic contact. The mean planes discussed are for the entire pyrene system rather than the individual rings.

Mean plane: C104 C105 C108 C111 C112 C115 to C204 C205 C208 C211 C212 C215

Angle between mean planes: 7.617 (0.382) degrees

Closest atomic contact: 3.2294 (0.0177) C117-C214 or 3.3621 (0.0196) C116-C216 Angstroms

Mean plane: C304 C305 C308 C311 C312 C315 to C404 C405 C408 C411 C412 C415

Angle between mean planes: 2.694 (0.419) degrees

Closest atomic contact: 3.3072 (0.0183) C314-C417 or 3.3007 (0.0202) C317-C414Angstroms

Table S1. Selected bond lengths (Å) and angles (deg) for $[Pt_4(\mu\text{-S-PrCh-}\kappa^3\text{-}C,N,S)_4]\cdot(CH_3)_2CO\cdot CHCl_3$ (**4**).

Bond lengths (Å)			
Pt1-C115 / Pt1-N118	2.035(14) / 2.002(10)	N(121)-C(122) / N(221)-C(222)	1.472(16) / 1.474(18)
Pt1-S120 / Pt1-S420	2.341(3) / 2.301(3)	N(321)-C(322)/ N(421)-C(422)	1.498(19) /1.41(3)
Pt2-C215 / Pt2-N218	2.078(13) / 2.007(11)	C(120)-S(120) / C(220)-S(220)	1.820(14) / 1.820(14)
Pt2-S220 / Pt2-S320	2.348(3) / 2.298(3)	C(320)-S(320)/ C(420)-S(420)	1.805(14)/1.797(15)
Pt3-C315 / Pt3-N318	2.001(12) / 2.002(10)	C(120)-N(121) / C(220)-N(221)	1.326(15) / 1.309(15)
Pt3-S120 / Pt3-S320	2.309(3) / 2.352(3)	C(320)-N(321)/ C(420)-N(421)	1.362(16)/1.323(16)
Pt4-C415 / Pt4-N418	2.002(13)/ 2.006(11)	N(119)-C(120) /N(219)-C(220)	1.284(14) / 1.305(16)
Pt4-S220 / Pt4-S420	2.301(3) / 2.357(3)	N(319)-C(320)/ N(419)-C(420)	1.300(15)/1.305(16)

Table S2. Selected bond angles (deg) for $[Pt_4(\mu\text{-S-PrCh-}\kappa^3\text{-}C,N,S)_4]\cdot(CH_3)_2CO\cdot CHCl_3$.

Bond Angles (°)			
C115-Pt1-S120	166.2(4)	C315- Pt3- S320	164.4(4)
C115-Pt1-S420	94.6(4)	C315- Pt3- S120	95.8(4)
N118-Pt1-C115	83.0(5)	N318-Pt3-C315	81.1(5)
N118-Pt1-C120	83.3(3)	N318- Pt3- S120	176.7(3)
N118-Pt1-S420	177.1(3)	N318- Pt3- S320	83.5(3)
S420 Pt1 S120	99.02(12)	S120- Pt3- S320	99.55(11)
C215-Pt2-S220	164.8(4)	C415- Pt4- S420	164.0(4)
C215-Pt2-S320	94.8(4)	C415- Pt4- S220	95.1(4)
N218- Pt2- C215	82.4(5)	N418-Pt4-C415	82.3(5)
N218- Pt2- S220	82.6(3)	N418- Pt4- S220	177.4(3)
N218- Pt2- S320	176.4(3)	N418- Pt4- S420	81.9(3)
S320- Pt2- S220	100.10(12)	S220-Pt4- S420	100.72(12)

Table S3. Hydrogen bonds for $[Pt_4(\mu\text{-S-PrCh-}\kappa^3\text{-}C,N,S)_4]\cdot(CH_3)_2CO\cdot CHCl_3$ (**4**)

D	H	A	d(D-H)/Å	d(H-A)/Å	d(D-A)/Å	D-H-A/°
N121	H121	O2	0.88	2.13	2.994(14)	167.2
N221	H221	O5	0.88	2.21	3.040(16)	158.3
C10	H10	O2	1.00	2.58	3.40(3)	139.4

Table S4. Inter-metal distances for $[Pt_4(\mu\text{-S-PrCh-}\kappa^3\text{-}C,N,S)_4]\cdot(CH_3)_2CO\cdot CHCl_3$ (**4**)

Inter metal distance	
Pt1 - Pt2	3.3494 (0.0008)
Pt1 - Pt3	3.7543 (0.0007)
Pt1 - Pt4	3.8237 (0.0007)
Pt2 - Pt3	3.7986 (0.0007)
Pt2 - Pt4	3.8179 (0.0007)
Pt3 - Pt4	3.3386 (0.0008)

Table S5. Flow cytometry analysis to determine the percentages of apoptotic cells, using Annexin V-FITC vs PI staining, after exposing A2780 human ovarian cancer cells to complex **3** and staurosporine. Concentrations used were IC_{50} and IC_{50} x 3 for complex **3** and 1 μg/mL for staurosporine (Sta), pre-incubation time in drug-free medium was 24 h and drug exposure time was 24 h.

Compounds	**Population (%)**			
	Viable	**Early Apoptotic**	**Non viable**	**Late Apoptotic**
3 (IC_{50} concentration)	98.56 ± 0.19	1.22 ± 0.18	0.02 ± 0.01	0.20 ±0.01
3 (3 x IC_{50} concentration)	98.60 ± 0.12	1.22 ± 0.13	0.01 ± 0.01	0.18 ± 0.01
Control	98.70 ± 0.93	1.36 ± 0.13	0.03 ± 0.02	0.34 ± 0.11

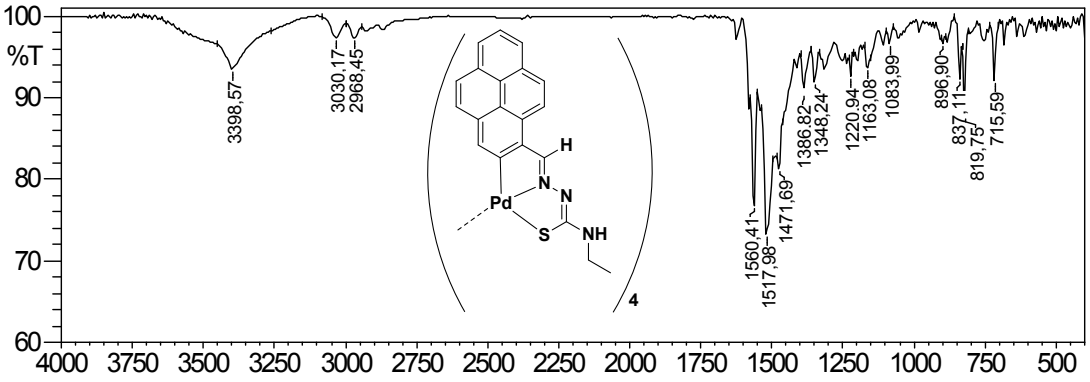

Figure S1. IR spectrum of complex **1**.

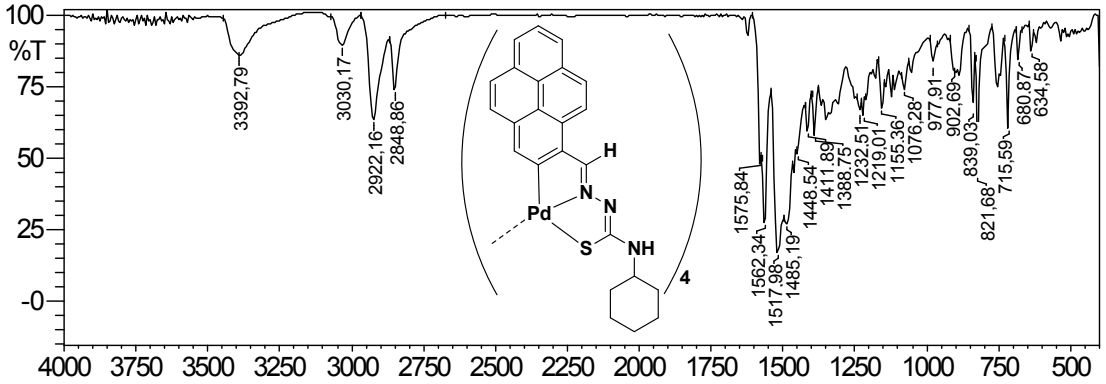

Figure S2. IR spectrum of complex **2**.

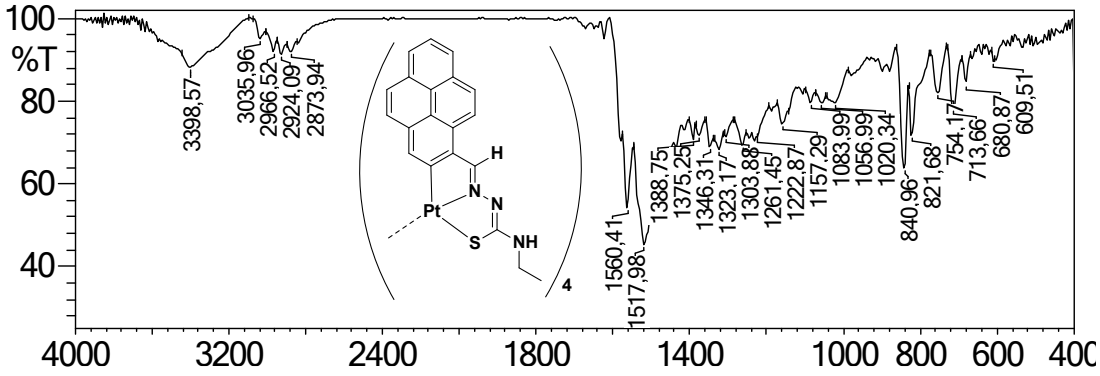

Figure S3. IR spectrum of complex **3**.

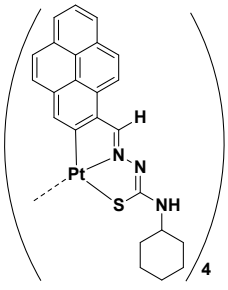

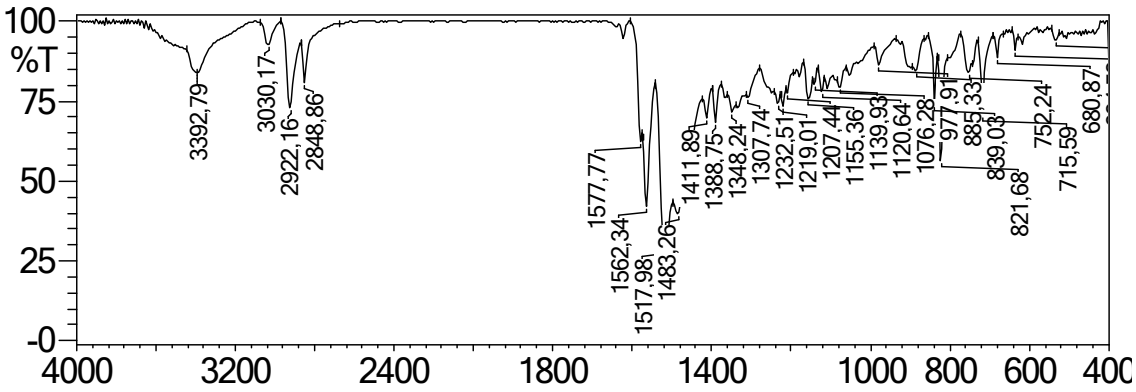

Figure S4. IR spectrum of complex **4**.

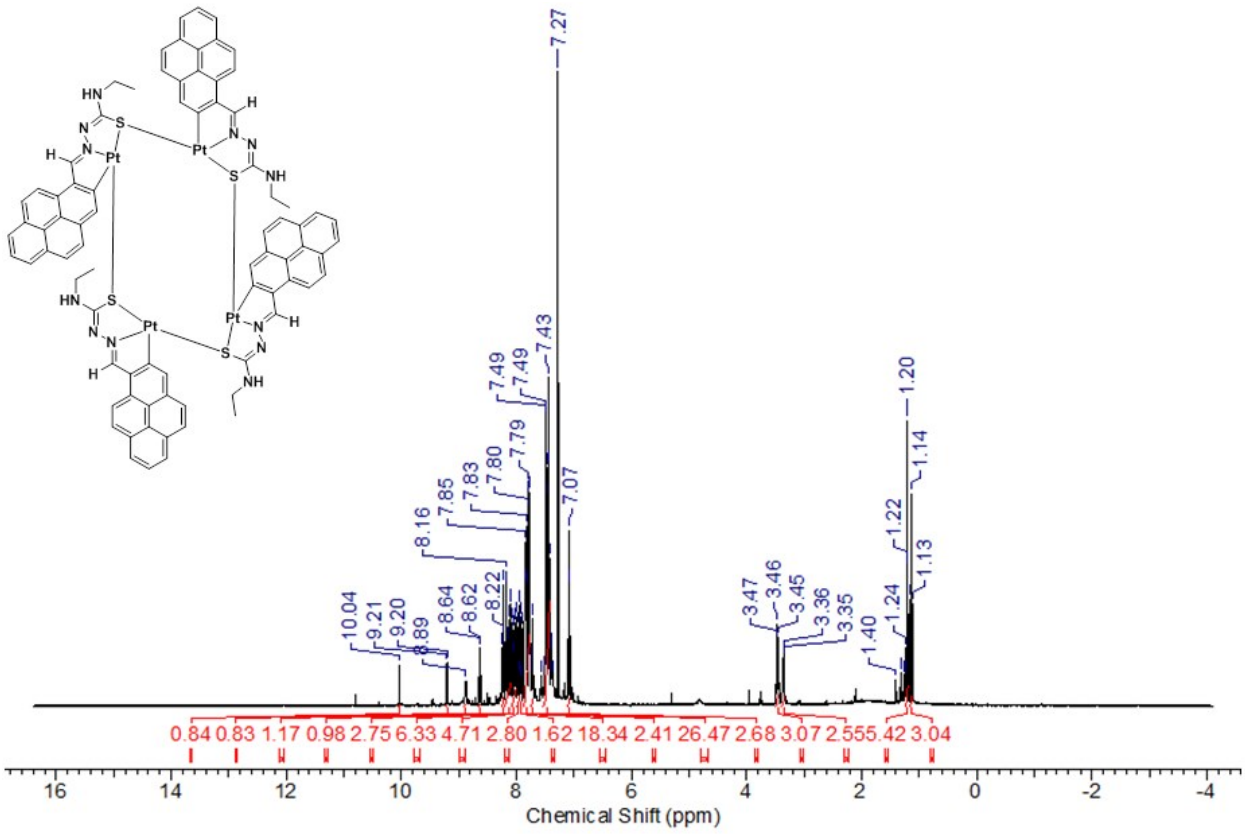

Figure S5. 500 MHz ^{1}H NMR spectrum of complex **3** in $CDCl_3$ as an example for the tetranuclear complexes. The spectrum shows two set of signals, suggesting that the tetranuclear possesses two monomeric units in different environments. The two sets of peaks in the aromatic region are assigned to the four pyrene units, while the two sets of aliphatic hydrogens represent the ethyl group substituent.

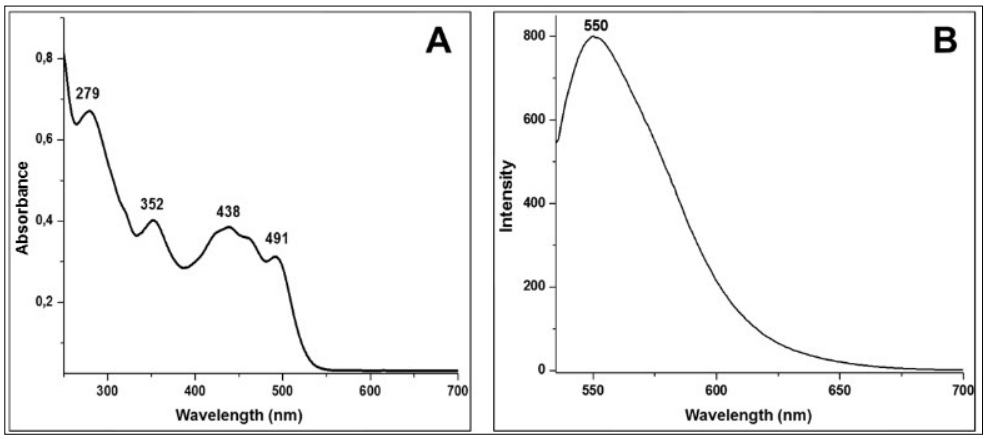

Figure S6. (**A**) UV-vis absorption spectrum of complex **1** in DCM, and (**B**) emission spectrum, λ_{exc}: 517 nm in DMSO (51 μM) at ambient temperature.

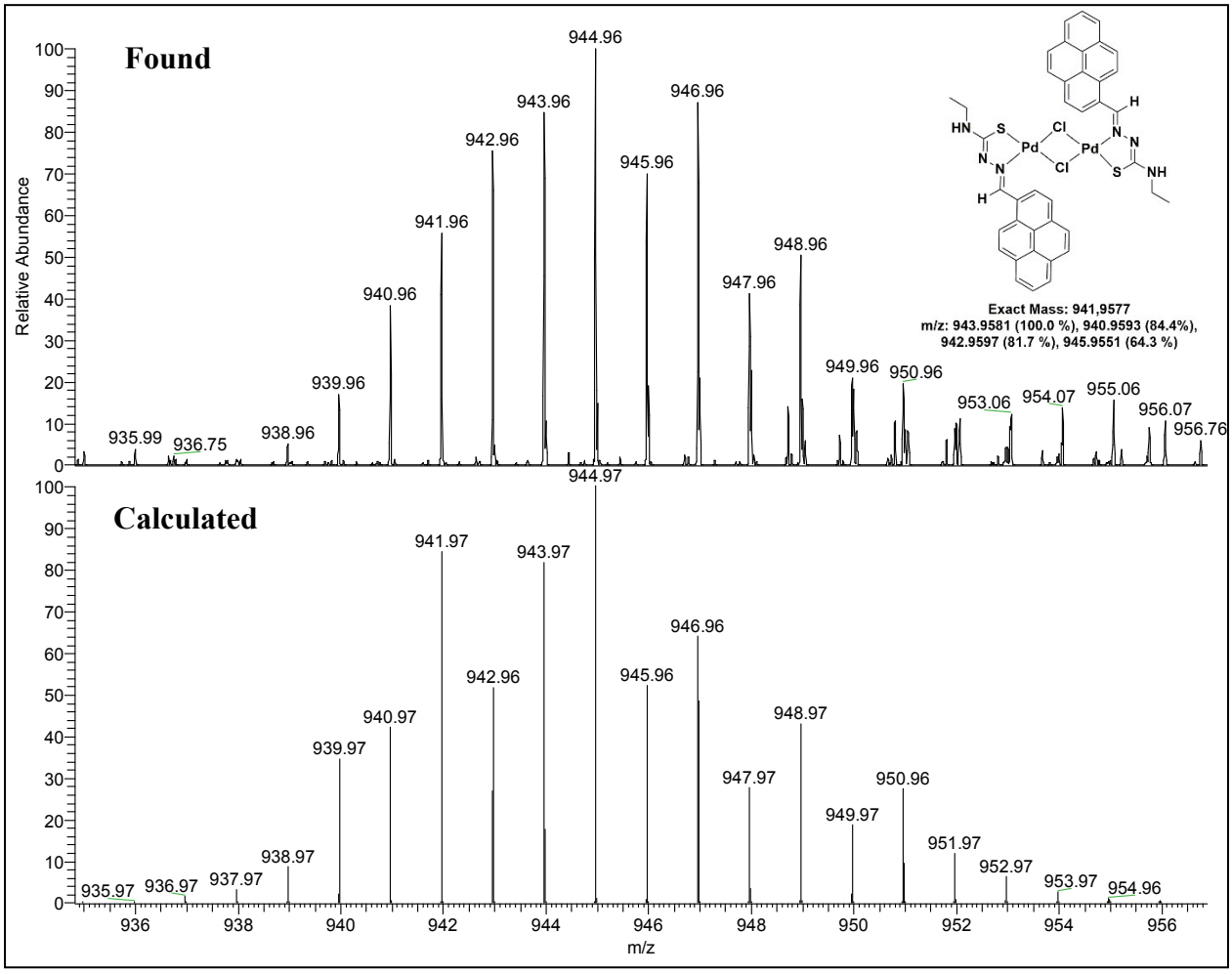

Figure S7. ESI-MS spectrum of the dimeric palladium complex **1** in positive mode at *m/z* calculated: 944.95 found: 944.96.

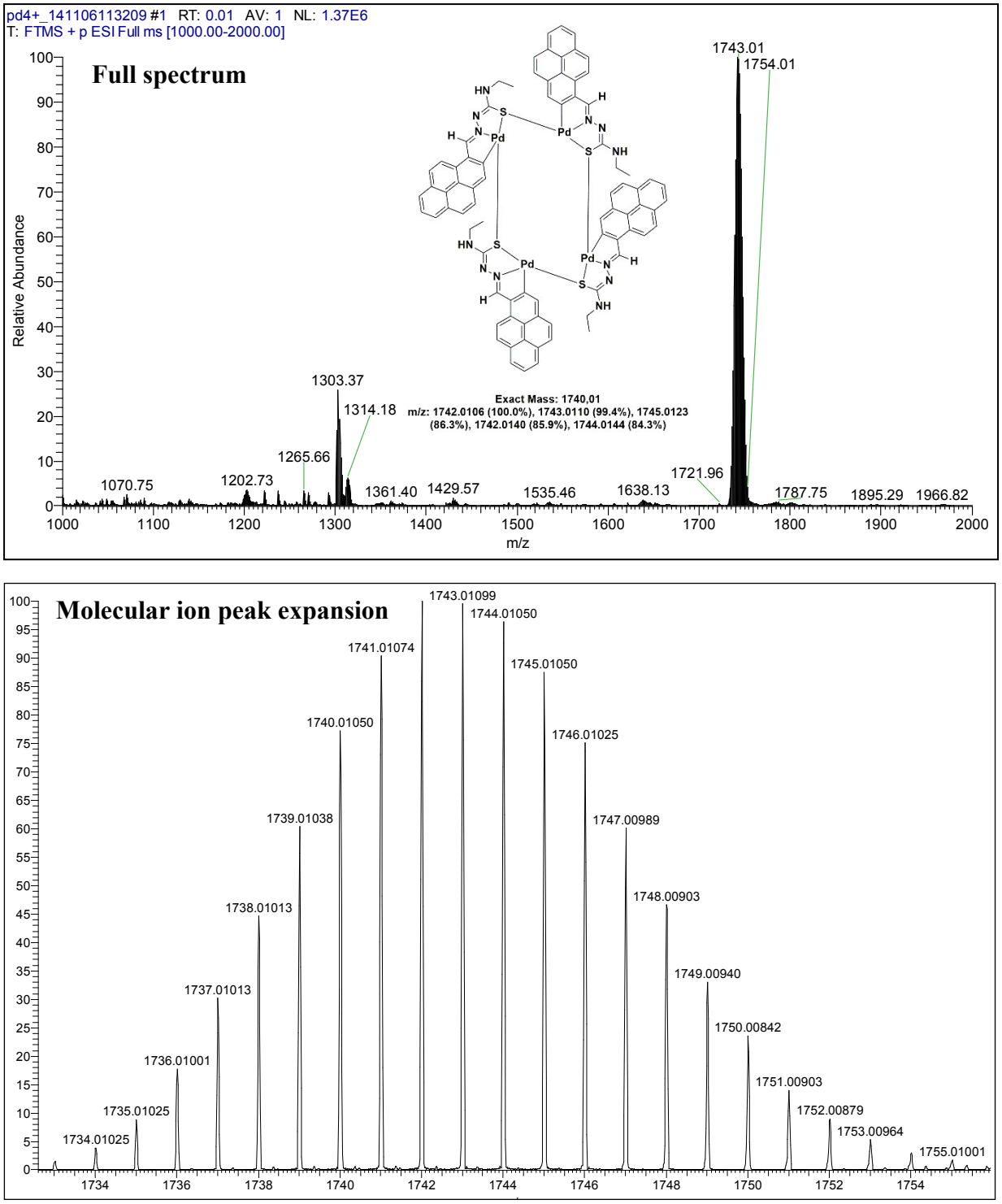

Figure S8. High resolution ESI-MS spectrum of complex $[Pd_4(\mu\text{-S-PrEt-}\kappa^3\text{-}C,N,S)_4]$ in DCM:MeOH (25:75 v/v) + 0.3% formic acid in positive mode at *m/z* calculated: 1743.0106 found: 1743.0109.

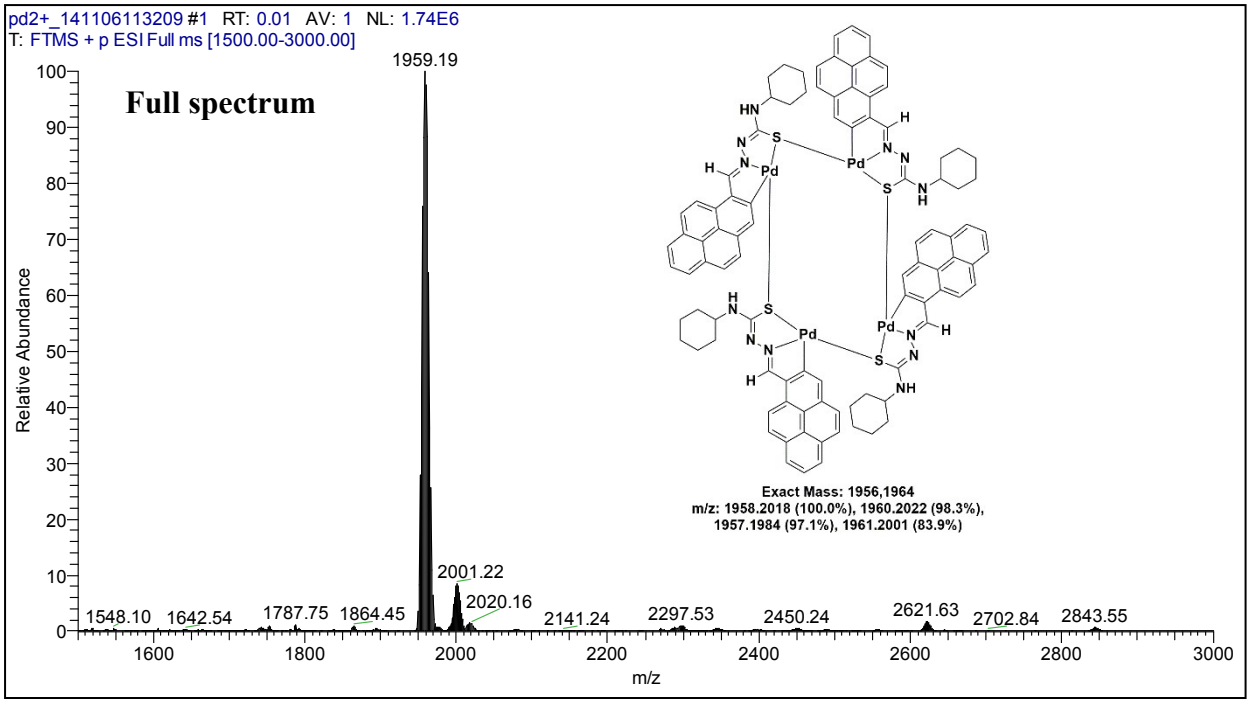

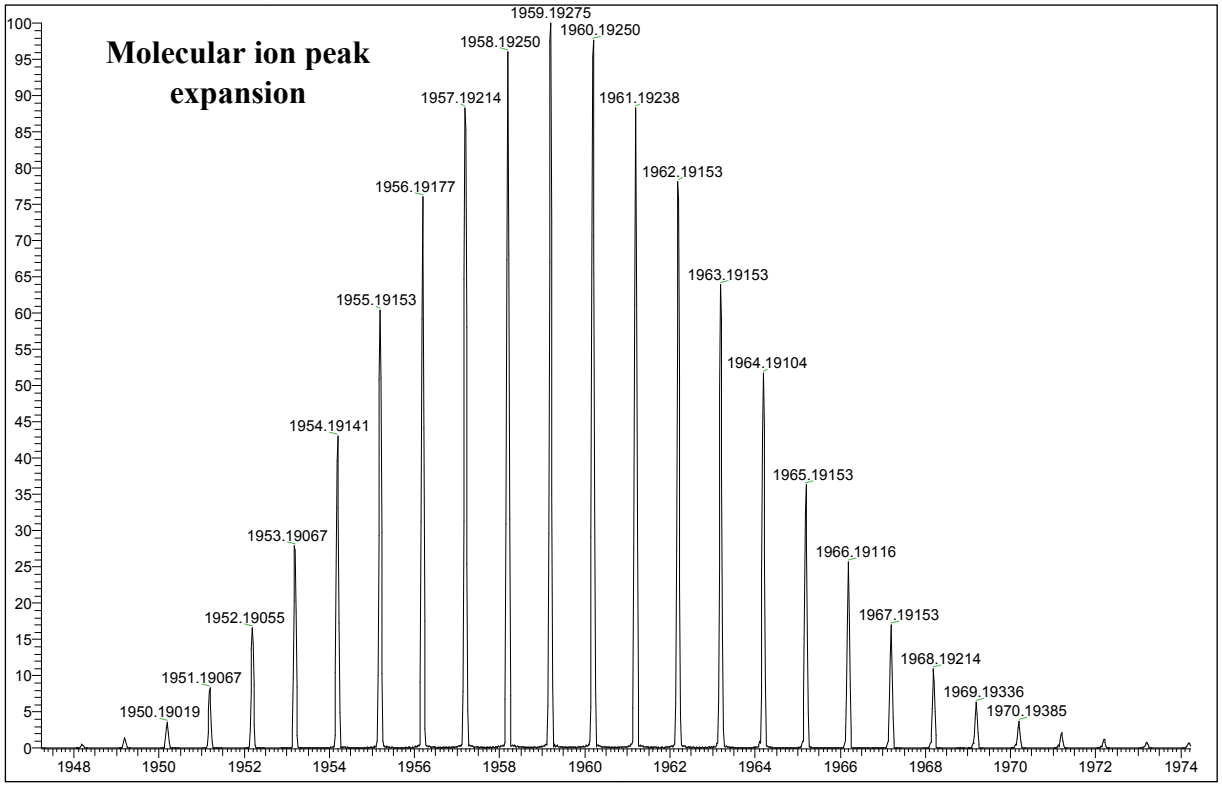

Figure S9. High resolution ESI-MS spectrum of complex $[Pd_4(\mu\text{-S-PrCh-}\kappa^3\text{-}C,N,S)_4]$ in DCM:MeOH (25:75 v/v) + 0.3% formic acid in positive mode at *m/z* calculated: 1959.2091 found: 1959.1927.

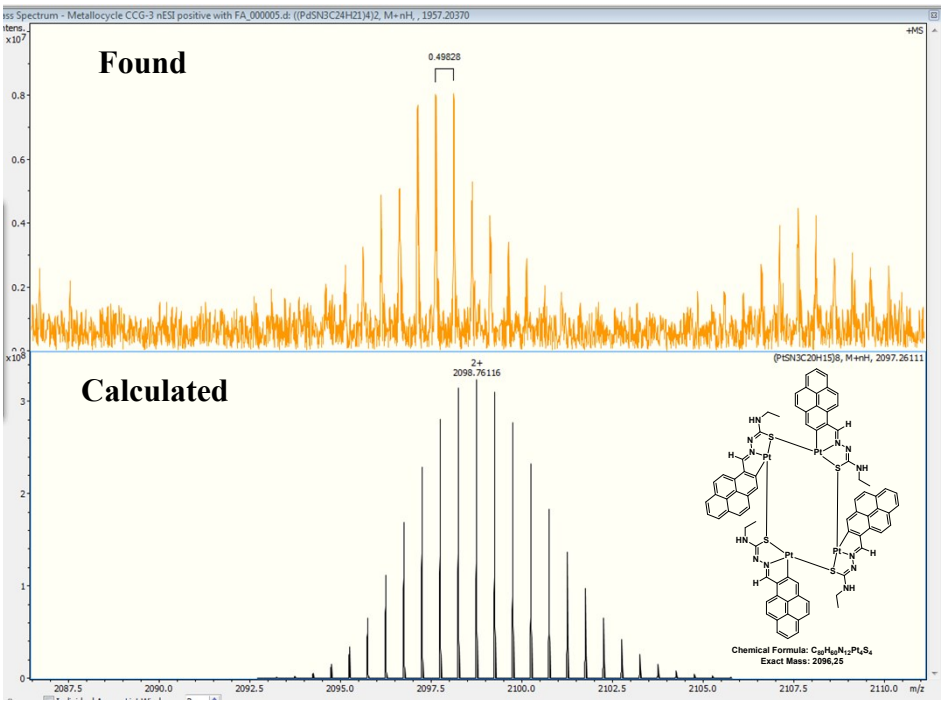

Figure S10. High resolution ESI-MS spectrum of complex $[Pt_4(\mu\text{-S-PrEt-}\kappa^3\text{-}C,N,S)_4]$ in DCM:MeOH (25:75 v/v) + 0.3% formic acid in positive mode.

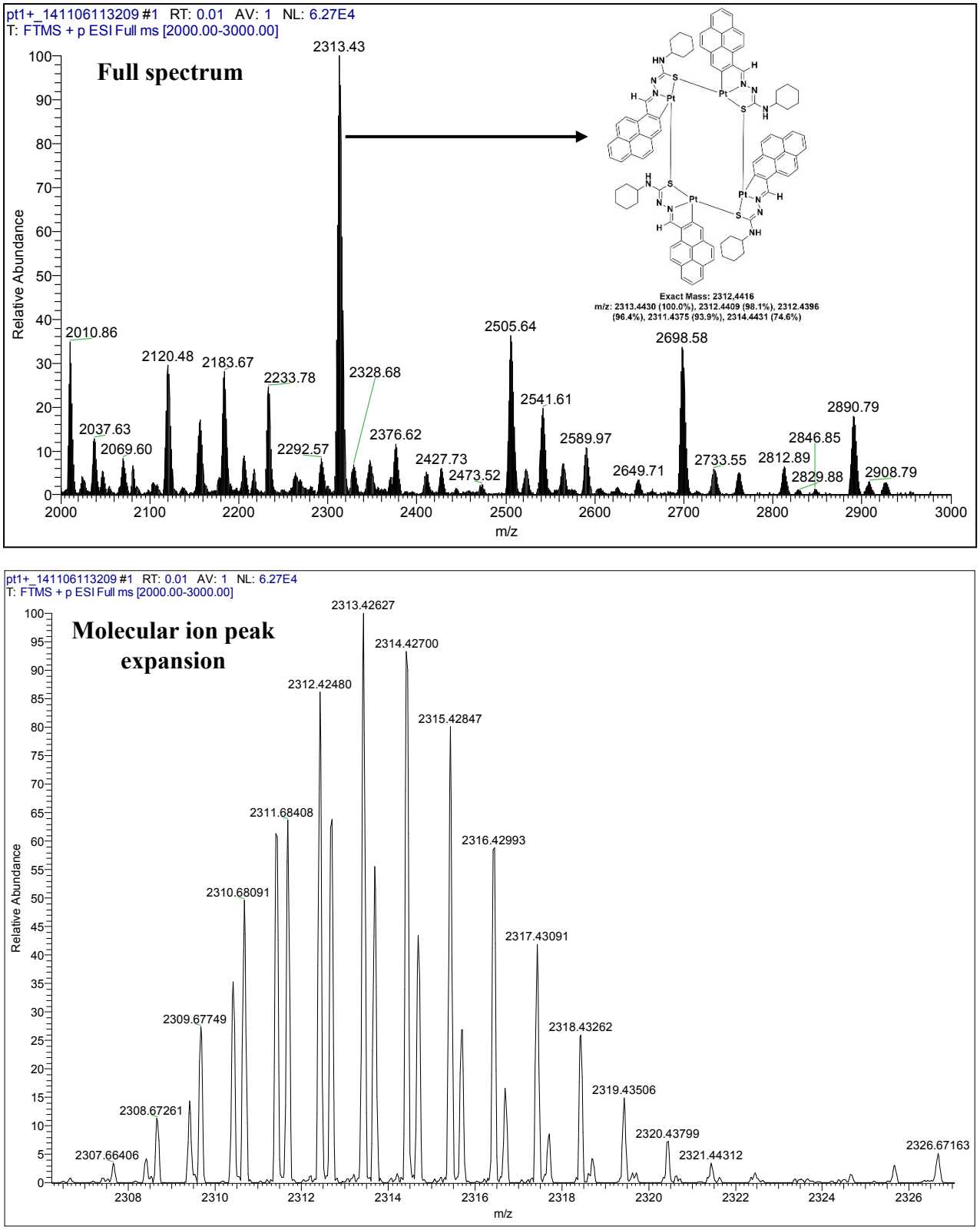

Figure S11. High resolution ESI-MS spectrum of complex [Pt_4(μ-S-PrCh-κ^3-*C,N,S*)$_4$] in DCM:MeOH (25:75 v/v) + 0.3% formic acid in positive mode at *m/z* calculated: 2313.4430 found: 2313.4262.

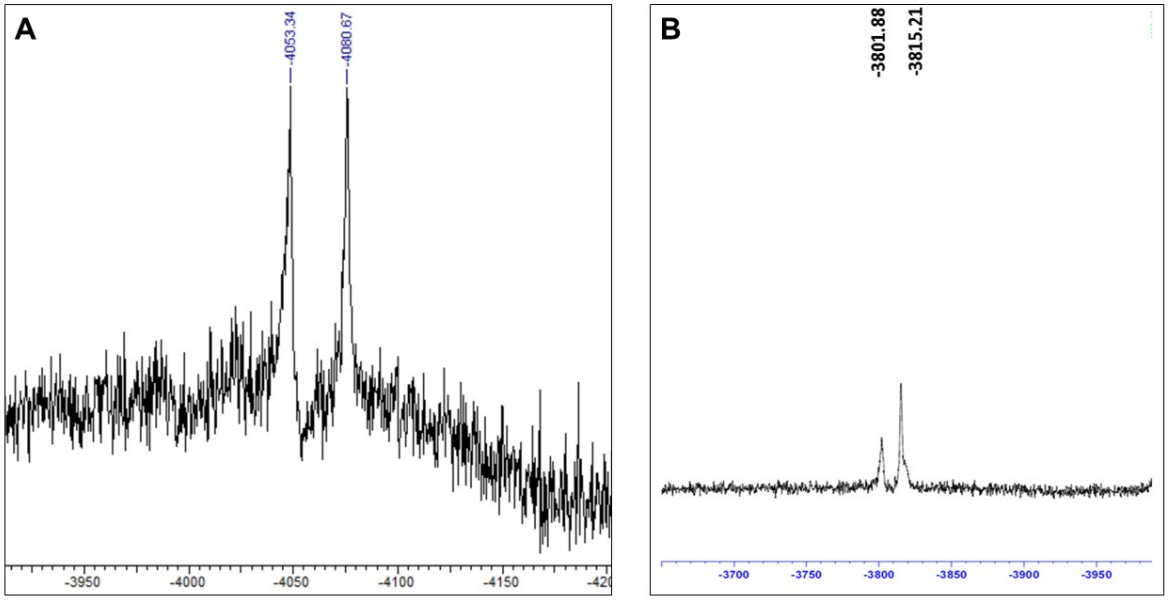

Figure S12. 500 MHz ^{195}Pt NMR spectra of A) complex **3**, and B) complex **4**, showing the presence of two non-equivalent monomers.

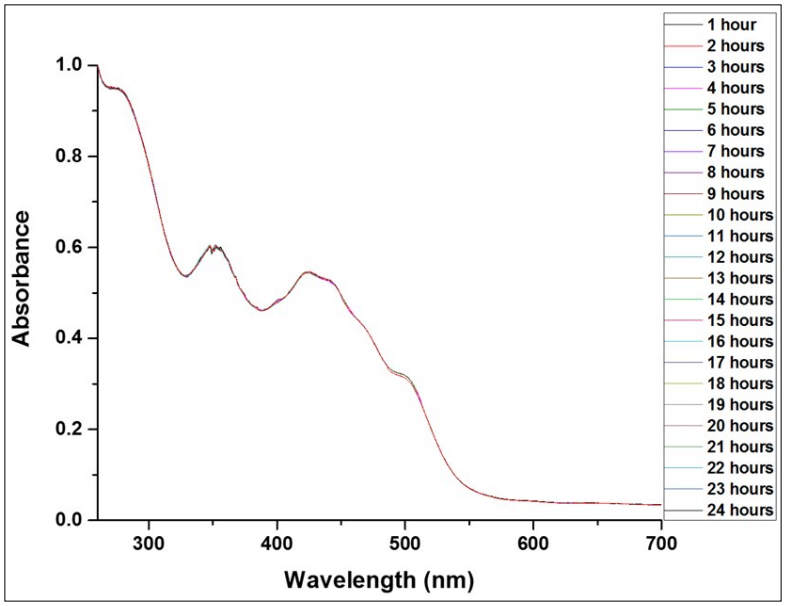

Figure S13. UV visible electronic absorption stability test for complex **1** in 95% H_2O, 5% DMSO at 50 μM. The experiment was carried out over 24 h at 298 K. The spectrum remained unchanged during the experiment time, showing that the compound does not hydrolyse under such conditions.